
Article:
Shehzad, MK, Forth, JP and Bradshaw, A (2020) Imposed loading effects on reinforced concrete walls restrained at their base. Proceedings of the Institution of Civil Engineers: Structures and Buildings, 173 (6). pp. 413-428. ISSN 0965-0911

https://doi.org/10.1680/jstbu.17.00179

Imposed Loading Effects on Reinforced Concrete Walls Restrained at Their Base

*__Muhammad Kashif Shehzad__, MEng, B.E (Civil), PE
PhD Student, School of Civil Engineering, University of Leeds, UK, orcid.org/0000-0002-2078-7651

__John P. Forth__, PhD, BEng, CEng, MIStructE
Professor, Chair in Concrete Engineering and Structures, Director of the Neville Centre of Excellence in Cement and Concrete Engineering,
School of Civil Engineering, University of Leeds, UK, orcid.org/0000-0002-4594-1475

__Adam Bradshaw__, MEng, CEng, MICE
Structural & Civil Engineering Director at BDP London, UK

*Corresponding Author, Room 1.09 School of Civil Engineering, University of Leeds, Woodhouse Lane Leeds, LS2 9JT, UK
cnmks@leeds.ac.uk, 01133437736

Abstract: This paper investigates the restraint of imposed strains in edge restrained members and in particular, experimentally illustrates the influence of vertical steel reinforcement between the restrained (wall) and the restraining (base) member on the mechanism of restraint development. The investigation constructed real scale reinforced concrete walls onto reinforced concrete bases and also illustrated why previous studies, which have mostly utilized steel members to restrain the imposed strain, are inappropriate for gaining an understanding of edge restraint as they fail to reflect the heat transfer between the wall and the base. Results revealed that the restraint increased in the presence of vertical steel reinforcement from 0.37 to 0.72. They also showed that restraint increases with time due to the steel reinforcement and decreases in its absence. A finite element analysis of the walls is also presented to highlight the significance of correctly incorporating the real time boundary conditions.

1. Introduction

Cracking in newly cast concrete subjected to restraint is a common phenomenon which is primarily attributed to the restraint of volume changes within the concrete. Immediately after casting and following peak hydration temperature, the concrete starts to exhibit volume change due to the concomitant processes of early age thermal contraction and shrinkage (both autogenous and drying). Some form of restraint to these volume changes is present in almost all practical scenarios. The restraint may be external and imposed by one or more of the

adjoining members; internal and be from the steel reinforcement present in the concrete; or result from thermal gradients / differential thermal strains, particularly those occurring in mass concrete structures (1). Once the free volume change of the concrete is restrained, tensile stresses will develop in the concrete which may lead to cracking, should the stresses exceed the tensile strength of the concrete. Cracks occurring due to the above mentioned phenomenon are mostly 'through cracks'. Design codes and construction practices present numerous measures to assist with the control of cracking; these include the lowering of the temperature during the hydration process, the provision of horizontal steel reinforcement, the provision of joints and the limiting of the length to height (L/H) ratio of each pour (2, 3). The mechanism of cracking due to external end restraint has been researched in detail and the theory of cracking due to restrained volume changes was developed based on the behaviour of members subjected to end restraint (4). However, little research has been performed on the behaviour of edge restrained members; most experimental research has been performed on reduced scale members with micro concrete and reduced bar diameters (5) or on mortar mixes (6-8), although recently, Micallef (9) conducted tests on full scale reinforced concrete walls subjected to a combination of flexure and edge restraint, where the restraint was imposed by a steel restraining base., Interestingly, the research that has been performed, suggests that the effects of end and edge restraint are quite different from each other (10, 11).

The mechanism of cracking due to restraint involves two important parameters a) magnitude of volume changes, b) degree of restraint. Whilst previous studies have focussed on ascertaining the factors involved in defining the magnitude of volume changes as well as on the restraint variation within the height of wall, the mechanism and factors involved in the formulation of edge restraint have not been experimentally identified and analysed in detail. One important reason for this may be the use in previous experimental investigations of a steel member as the restraining base; although this may simulate edge restraint, the behaviour of the concrete base in terms of thermal contraction, heat transfer and the role of the steel dowels which are continuous from the base into the wall cannot realistically be depicted by the steel members. It must be noted also, that although external restraint has been categorized as Edge and End restraint; in practice, a combination of edge and end restraint is also commonly witnessed (1).

Tensile stresses developed in concrete members subjected to edge restraint are believed to be proportional to the magnitude of the restrained strain. The restrained strain (ε_r) is the

strain prevented from occurring due to the presence of the edge restraint and is the product of the degree of restraint (R) and the free strain (ε_{free}) likely to occur in the concrete in the absence of a restraint. Degree of restraint varies between 0 (for no restraint) and 1 (for full restraint) and is defined as the ratio of restrained strain to free strain. Currently, it is suggested that the degree of restraint can be calculated or ascertained using the guidance / equations given by ACI Committee 207 (12) and BS EN 1992-3 (13); the method of estimation of edge restraint given in CIRIA 660 is similar to the one given in the ACI design code. Nilsson (14) also suggested several expressions for the calculation of edge restraint for a typical case of a wall on a slab. The ACI method is based on the work by Carlson and Reading (15); it was subsequently improved in light of the work by Emborg (16). Using the ACI approach, the restraint at the joint is calculated from the ratio of the axial rigidity of both members as given in Equation 1. Research by Stoffers (5) and Kheder, Al-Rawi (8) indicates that the degree of restraint varies along the height of wall and is a function of the wall aspect ratio. The ACI also varies the restraint over the height of the wall by incorporating the length to height ratio (L/H), height of the wall (H) and height (h) of the point above the joint at which restraint is being considered. Since the modulus of elasticity of new concrete, E_c increases with time, then according to this equation, the value of restraint at the joint should decrease with the passage of time. No experimental evidence of change in restraint with time has been provided by researchers in the past, however, Micallef (9) did find that the restraint increased with time, proposing that this was due to the reduction of wall stiffness after cracking.

$$R_j = 1/(1 + \frac{A_g E_c}{A_f E_f}) \qquad 1$$

where;

R_j = Degree of restraint at the joint

A_g = Gross area of concrete cross section

A_F = Cross sectional area of foundation or other restraining member

E_c = Modulus of elasticity of restrained member concrete

E_f = Modulus of elasticity of foundation or restraining element

Annex L to BS EN 1992-3 (13) proposes a number of restraint factors (these have been reproduced from BS 8007 (17)). The Annex provides a value of 0.5 for the degree of restraint and suggests that this will remain unchanged over the height of the wall. Similarly, BS 8110-2 (18) suggested that the restraint factor lay between 0.6 and 0.8, for a wall cast on a massive concrete base. However, Bamforth (3) found that a difference in degree of restraint of 0.1 from

the Eurocode suggested value will affect the level of restrained strain by 20% and, therefore, suggested a more rigorous estimation of restraint factors is necessary. Klemczak and Knoppik-Wróbel (19) carried out a comparative study of these three methods and concluded that; the Eurocode approach is useful only when assuming that the restraining member does not deform; the ACI approach is simple and easy to use with results being similar to those obtained from numerical analysis, however, the approach focuses mainly on the volume changes due to thermal effects, since it has been developed for mass concrete; the method given by Nilsson (14) is quite complex and a little difficult to use - also, its application is limited and only applicable to wall elements having aspect ratios of less than 5.

There is a consensus among researchers in this field that the degree of restraint is maximum at the joint between the restrained and restraining member and at the centreline of the wall, and that the restraint reduces over the height and length of the wall (3, 5, 7, 14, 15). However, Micallef (9) noticed that the maximum value of restraint may exist at some point above the mid height of the wall, although this may be influenced by the test procedure that was adopted. Stoffers (5) and Schleeh (20) conducted tests on micro concrete walls having different L/H ratios and cast on a steel base. They identified the significance of taking into account the curvature induced in the restraining member due to the contraction of the wall when calculating the restraint factors. A similar approach for analysing edge restrained walls was recently adopted by Micallef (9), however, full scale reinforced concrete walls were investigated in the latter case. In the latter case, restraint was induced through the use of shear connectors welded onto the steel universal column which was used as the restraining base. To prevent the universal column from developing any curvature, actuators and load cells were installed beneath the steel base and an upward pre-load was applied which introduced hogging action into the base and wall. In all of the above cited research, restraint was imposed to the edge of the restrained walls, however, the influence of the volume changes taking place in the wall on the restraining member could not be ascertained. In most practical cases, a wall is cast onto an existing concrete member and a certain amount of vertical steel reinforcement is present at the joint. As of yet, the contribution of this reinforcement in defining the degree of restraint cannot be assessed from the existing research / the existing design guidance expressions.

This paper aims to identify the influence of vertical steel reinforcement on the behaviour of edge restrained reinforced concrete walls by specifically focusing on the degree of restraint,

number and width of cracks and the role of the edge restraining element. It also highlights the shortfalls of using a steel member as a restraining base for edge restrained reinforced concrete walls.

2. Experimental Program

2.1. Introduction

In light of the shortfalls of previous research mentioned above, an experimental research programme looking at the behaviour of edge restrained reinforced concrete walls has been undertaken. This research focuses on 1) highlighting the importance of using a reinforced concrete base in order to correctly understand the phenomenon of edge restraint and 2) determining the role of the vertical steel reinforcement dowels extending from the base into the walls on the mechanism / development of restraint. The experimental study primarily considers tests on four reinforced concrete walls cast onto previously constructed and hardened reinforced concrete bases. Tests on two walls have been completed and their results are presented in this paper; the remaining two tests are currently in progress (In the ongoing tests, the wall thickness has been reduced to analyse the influence of the axial rigidity of both members on the degree of restraint). During the period of testing, the average temperature in the laboratory varied between 14 and 24°C, and the average relative humidity ranged between 46 and 62 %.

2.2. Test Set Up

Each test comprised of two phases. In phase 1, the reinforced concrete base slab was cast and cured for up to 28 days. In phase 2, once the slab was at least 28 days old, the wall was cast on the existing slab; hence, the existing slab imposed a restraint to the volume changes occurring in the newly cast wall. The detailed dimensions of both the wall and slab are given in Figure 1. The wall had a length to height ratio (L/H) of 4, which is similar to the walls tested by Stoffers (5) and representative of the range of commonly used aspect ratios in practice. In both tests, the walls had a larger cross sectional area (240000 mm^2) than that of the base slab (204000 mm^2). The strains and temperatures in both the wall and slab were monitored for a period of eight weeks after the wall had been cast. Strains were measured using DEMEC gauges, while temperatures were monitored using K type exposed welded tip thermocouples. For these tests, it was decided to prevent the development of curvature in the base slab, hence, both ends of the slab were bolted to the strong floor of the laboratory using two-off 50 mm

diameter steel studs as shown in Figure 1. An 8 mm thick steel plate was also placed on top of the slab ends to distribute the force applied by tightening the nuts. The upward deflection at the slab ends was monitored using analogue deflection gauges at both ends of the base. A constant value on these deflection gauges was maintained throughout the test by tightening the nuts whenever any upward deflection was detected during the test period. This adjustment was performed a maximum of 3 times during the test and the maximum upward deflection observed was 0.05 mm.

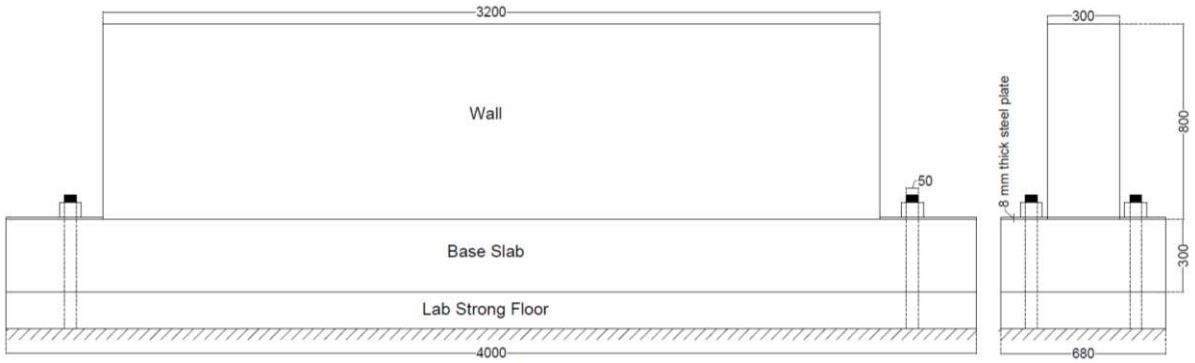

(a)

(b)

Figure 1. The test set up: (a) Elevation and cross section of the wall and base (dimensions are in mm); (b) a view of the tested wall

2.3. Design of Specimens

In the process of designing the specimens and in addition to the points already mentioned above, it was deemed important to implement the following further considerations:-

a. The length (L) of the walls should be sufficient to allow the development of at least two primary cracks (according to the guidance on crack spacing available in the literature).
b. The concrete mix should be designed to provide a significant thermal drop (from peak temperature) and shrinkage.
c. The walls should be sufficiently high to allow any variation in restraint over the height of the wall to materialise.
d. The base should be prevented from developing curvature due to the shrinkage and thermal contraction occurring in the wall (the influence of doing this on the restraint profiles are considered and reviewed below using FE analysis).

The details of the reinforcement provided in the wall as well as in the base for each test and the concrete cover are shown in Figure 2. The base slab was reinforced, on both top and bottom faces, longitudinally with 12 mm diameter bars spaced at 100 mm and in the lateral direction with 8 mm diameter bars spaced at 200 mm. In the first test, the wall had 10 mm vertical steel reinforcement bars spaced at 1040 mm (used merely to hold the horizontal bars in place) which meant that there were only eight 10 mm (ρ_v = 0.07%) dowels at the wall – slab joint. In the second test, 16 mm diameter steel bars spaced at 150 mm (ρ_v = 0.9%), were used as the vertical steel reinforcement in the wall. Both walls were reinforced horizontally with 10 mm diameter bars with a spacing of 180 mm in each face.

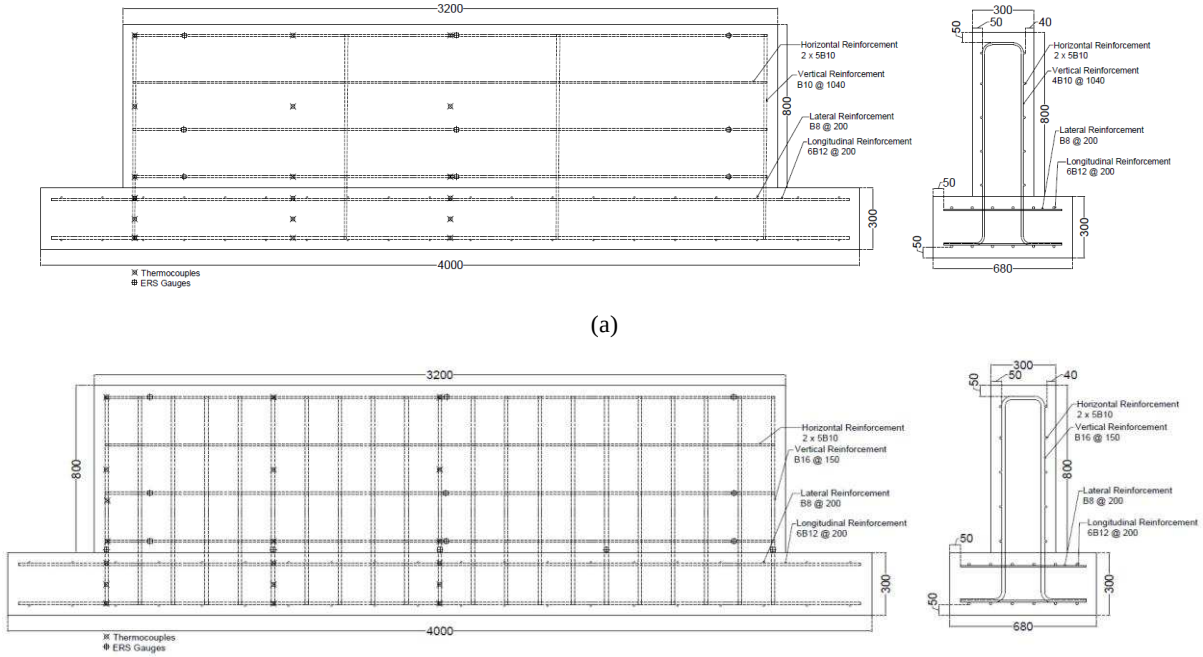

Figure 2. Details of steel reinforcement, cover and location of thermocouples and ERS gauges: (a) Test 1; (b) Test 2

2.4. Material Properties and Instrumentation

The concrete mix used in this study had a water to cement ratio of 0.45. The mix composition is given in Table 1. One cubic meter of ready-mixed concrete was procured from Hanson Concrete, Leeds each time an element was cast. The compressive strength (f_c), splitting tensile strength ($f_{ct,sp}$) and the modulus of elasticity (21) of each batch of concrete were determined in the laboratory. All the specimens were moist cured inside a curing room (99% relative humidity). The cube compressive strength ($f_{c,cube}$) of each concrete mix was determined using 100 mm cubes and the splitting tensile strength was obtained using 150 x 300 mm cylinders; strengths were obtained at 3, 7, 14 and 28 days. Figure 3 shows the development of compressive strength and indirect tensile strength with time for each batch of concrete. The cylinder compressive strength ($f_{c,cyl}$) and modulus of elasticity of each mix were also obtained using 150 x 300 mm cylinders at the age of 28 days. To determine the direct tensile strength (f_{ct}) of concrete, concrete bobbins were used; these direct strengths were compared with the indirect strengths obtained from the splitting tensile strength tests and all 28-day strengths along with the variation between the direct and indirect values are shown in Table 2. BS EN 1992-1-1 (22) suggests that direct or axial tensile strength should be taken as 90% of the splitting tensile strength whereas the data in Table 2 indicates that the direct tensile strength obtained is approximately 65% of the splitting strength. Although testing concrete bobbins for direct tensile strength has its inherent inaccuracies, it appears that the factor of 0.9 as suggested by the Eurocode is perhaps too high. Four prisms (75 mm x 75 mm x 200 mm) for each batch of concrete were used to obtain the free drying shrinkage. In all cases, these prisms were cured under the same environmental conditions as their respective wall and slab elements. Surface strains on both the wall and base were measured immediately after the removal of the formwork using the 150 and 400 mm DEMEC gauges. The temperature development in both wall and slab were monitored using thermocouples installed at different locations over the height and length of both members as shown in Figure 2 above and Figure 4 below. Owing to symmetry, temperatures were only monitored in one quarter of each member. Electrical resistance strain (ERS) gauges were also installed on selected steel bars, as indicated in Figure 2, to monitor the strains occurring in the steel reinforcement bars.

Table 1. Composition of the concrete mix

Ingredients	Quantity (kg/m^3)
Cement (CEM I)	385
Water	175
Fine Aggregate	730
Coarse Aggregate	1364
Admixture	VS1000

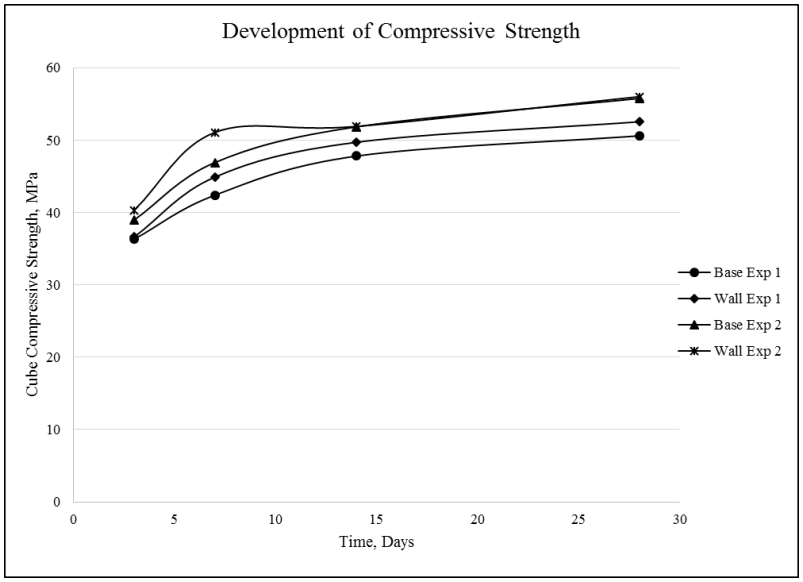

(a)

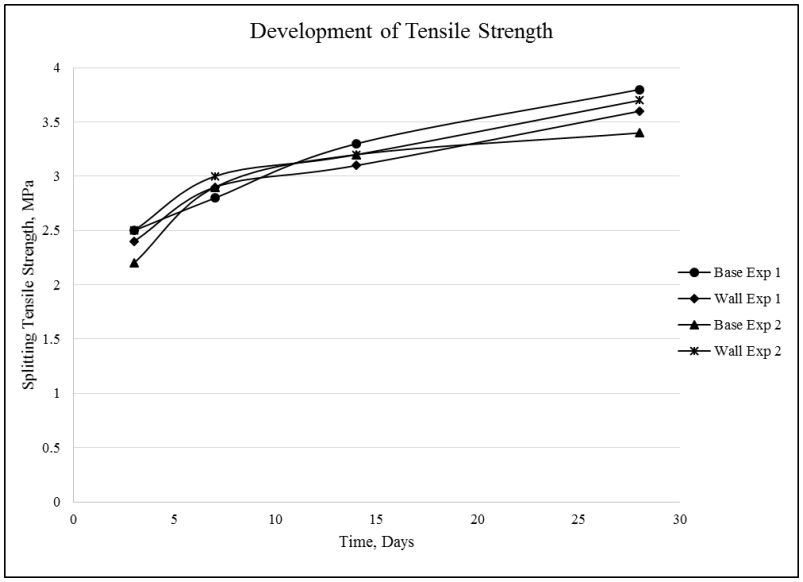

(b)

Figure 3. Development of concrete strength for each mix: (a) Compressive strength; (b) Tensile strength

Table 2. Comparison of splitting and direct tensile strength

Concrete Mix	Splitting tensile Strength (MPa)	Direct tensile strength (MPa)	Variation (%)
Base 1	3.8	2.8	26.3
Base 2	3.6	1.9	47.2
Wall 1	3.4	2.1	38.2
Wall 2	3.7	2.5	32.4

2.5. Test Procedure

Initially, the reinforced concrete slab was cast; the formwork for the slab was removed two days after casting. Thereafter, it was covered with wet Hessian sheets and cured for a period of 14 days. DEMEC studs were attached to the concrete on both longitudinal faces of the slab and the strains were recorded using 150 mm DEMEC gauge. Temperature recordings were logged every 15 minutes. Twenty eight days after casting the slab, the wall was cast using formwork insulated with 50 mm thick polyisocyanurate (PIR) thermal insulation sheets (which have a thermal conductivity of 0.022 W/m.K) to prevent heat loss to the atmosphere. In the first test, the wall formwork was removed 48 hours after casting whereas, in the second test it was removed after 20 hours. DEMEC studs were installed on the wall surface within 2 hours and then first readings were taken. Surface strain monitoring started immediately after the removal of the formwork and continued for the duration of the test. Immediately prior to the removal of the wall formwork, the bolts were checked to ensure that the base slab was uniformly in contact with the floor. In order to maximize the early age thermal contraction and shrinkage the wall was not cured after the removal of the formwork. Detailed monitoring of the surface strains and the appearance of cracks in each wall was carried out for a period of eight weeks after the removal of the formwork. In the case of the first wall, no primary cracks were observed during the test except for a few irregularly inclined plastic shrinkage cracks. However, in the second test, the first crack in the wall occurred 51 days after casting; the wall was monitored for a further four weeks after this. Crack widths were measured perpendicular to the crack using a portable microscope with a magnification of 40 and a precision of ±0.02 mm.

3. Results and Discussion

3.1. Temperature Development

The temperatures developed in both the wall and the base are presented in Figure 4. The vertical dotted lines in Figure 4 depict the time of formwork removal. A sharp decline in temperature can be seen in both tests on removal of the formwork. Temperatures within the concrete dropped to ambient values after 72 to 80 hours from initial casting. Temperature drop remained gradual except at the time of formwork removal. In test 2, a steep decline in temperature on removal of the formwork can be seen compared to test 1. The maximum temperature reached in test 1 was 55.4°C and in test 2 it was 50.5°C; both of these values occurred near the top of wall along the wall centreline. Near the free edge, the maximum temperature occurred at the mid height of the walls (and was 52.1°C in test 1 and 49.5°C in test 2) which were quite similar to the temperatures recorded near the top of the walls. However, temperatures observed in the wall close to the joint between the wall and the base were significantly lower than those at the higher locations in the wall. The temperature drop (T_1) from the peak to the ambient temperature in both tests was almost similar. The temperature drop at the centre of the wall was 33.5°C in test 1 and 33.3°C in test 2. The temperature drop obtained from CIRIA 660 for a 300mm thick wall, having a cement content of 380 Kg/m^3 is 30°C which is slightly less than the values obtained in these tests. Due to the increase in wall temperature during hydration, a rise in temperature in the base was also observed; this was greater close to the joint with the wall and lesser towards the bottom of the base, near the floor. This suggests that a significant amount of heat is transferred from the wall to the base in the region of the joint. This is in line with the observations of Bamforth (11) who predicts that this heat loss is the reason that the maximum crack width occurs at some height above the joint.

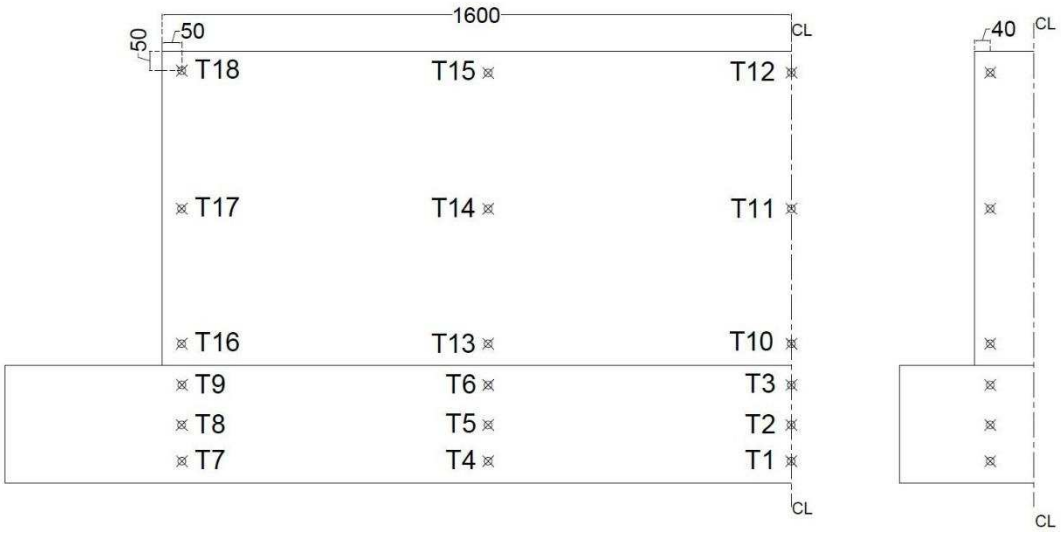

(a)

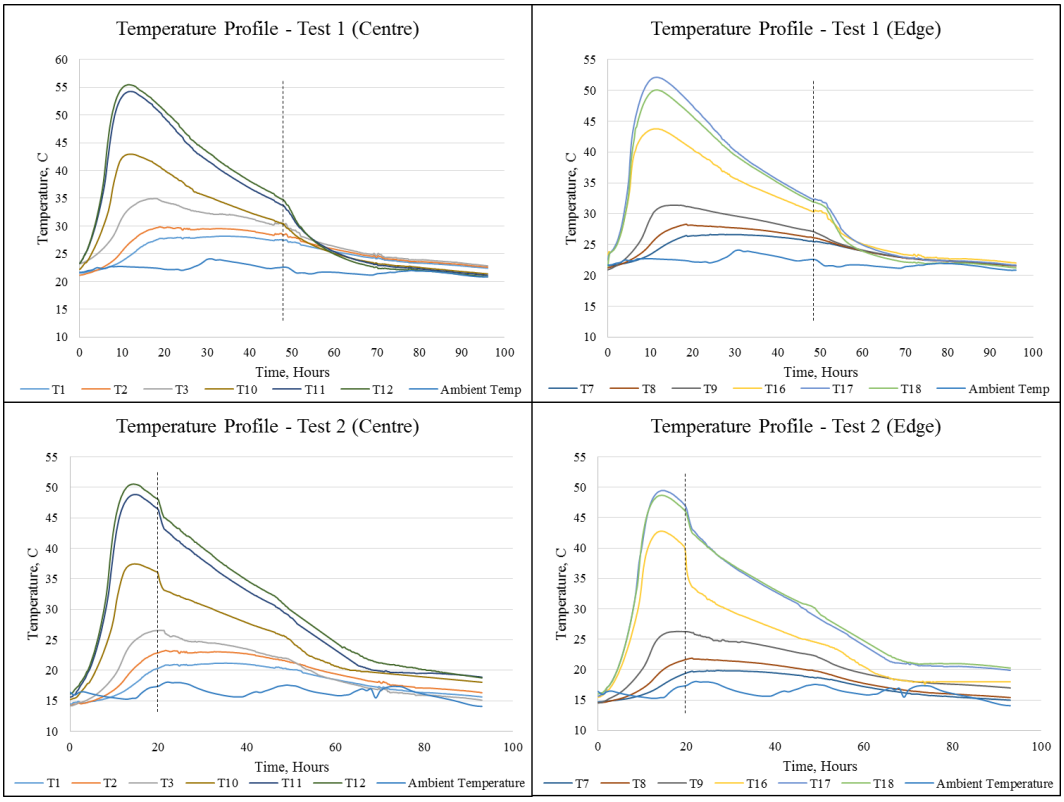

(b)

Figure 4. Temperature development after casting of the wall: (a) Location of thermocouples; (b) Temperature profiles

3.2. Unrestrained Shrinkage Comparison and Estimation

The unrestrained or free shrinkage measured from the concrete prisms was compared to the shrinkage predicted by the ACI model, Bazant Baweja B3 model, CEB FIP Model code 2010 model and the Eurocode model (see Figure 5). From Figure 5, it can be seen that the experimentally observed unrestrained shrinkage observed in both tests was most accurately

predicted by Model Code (23). Therefore, knowing the concrete properties and the notional size of the wall and base, the unrestrained shrinkage for both members was estimated using the Model Code (23) in the calculation of the restraint factors. The thermal strain was calculated by multiplying the thermal drop measured by the thermocouples with the coefficient of thermal expansion of the concrete. The coefficient of thermal expansion of concrete (α_c) was not measured experimentally, however, a comparative analysis was carried out using three values i.e. α_c = 9, 10 and 11 με/C. From this comparison, it was found that the degree of restraint slightly increases with an increase in the value of α_c, however, the variation of restraint over the height and with time remains similar. It was, therefore, decided to use the value of α_c = 10 με/C as recommended by BS EN 1992-1-1 (22) and Bamforth (3) in CIRIA 660 when a limestone aggregate is used. The sum of the thermal and shrinkage strain gave the free or unrestrained strain in the wall which was used to calculate the restrained strain and the degree of restraint.

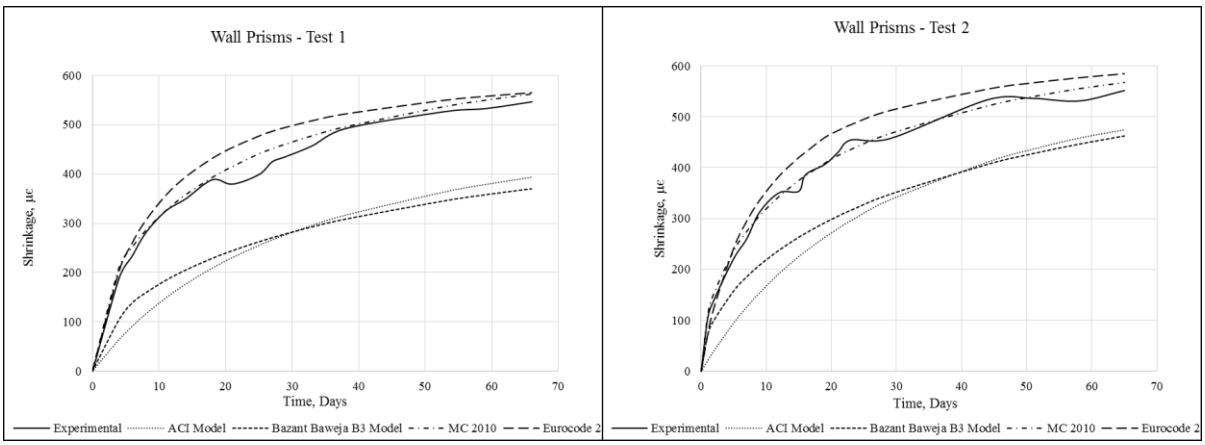

Figure 5. Comparison of experimentally obtained shrinkage with different shrinkage prediction models

3.3. Influence of Wall on the Shrinkage in Base

As mentioned above, the heat generated by the wall after casting meant that the base also underwent thermal changes along with the wall and an expansion in the base was observed after the wall was cast followed by a subsequent contraction (see Figure 6). Based on the observed shrinkage in the base prior to the casting of the wall, the shrinkage strain likely to occur in the base in the absence of wall was extrapolated and compared to the actual strain exhibited by the base once the wall was cast in place (see Figure 6). From Figure 6, it can be seen that in test 1, where a negligible amount of steel reinforcement (ρ_v = 0.07%) was present at the joint, the volume changes occurring in the wall increased the base contraction as compared with the strain predicted to occur in the base in the absence of the wall. However,

in test 2, when the reinforcement dowels were present, the contraction in the base was found to be less than that expected to occur in the absence of wall.

These results confirm that the action of the newly cast wall is to induce volume changes in the concrete base primarily due to the heat transferred from the wall to the base during the hydration of the concrete in the wall. This interaction between the base and the wall is clearly difficult to quantify when steel members are used as a restraining base; yet it is extremely important. In test 1, the base exhibited more strain than was anticipated from its behaviour before the wall was cast; in test 2 the induced volume change in the base was restrained due to the presence of the vertical steel reinforcement possibly because the steel reinforcement bears against the contracting concrete and restrains the free strain. It can, therefore, be inferred from the results that the dowels enhance the stiffness and thus the restraint imposed by the base on the wall.

The restrained strain at the bottom of the wall is the combination of the restrained strain calculated for the wall and the restrained strain in the base. Therefore, in the experimental evaluation of the degree of restraint, it is important to take into account the strain restrained from occurring in the base slab in order to correctly ascertain the degree of restraint imposed on the wall. The presence of the steel reinforcement at the joint has clearly increased the effective stiffness of the base as a result of the enhanced shear transfer between wall and base. However, currently available guidance for the estimation of the restraint factor does not incorporate this steel reinforcement ratio. The amount of vertical steel reinforcement present at the joint between the restrained and the restraining members is therefore an important contributory factor towards the formulation of restraint and needs to be incorporated within the design guidance.

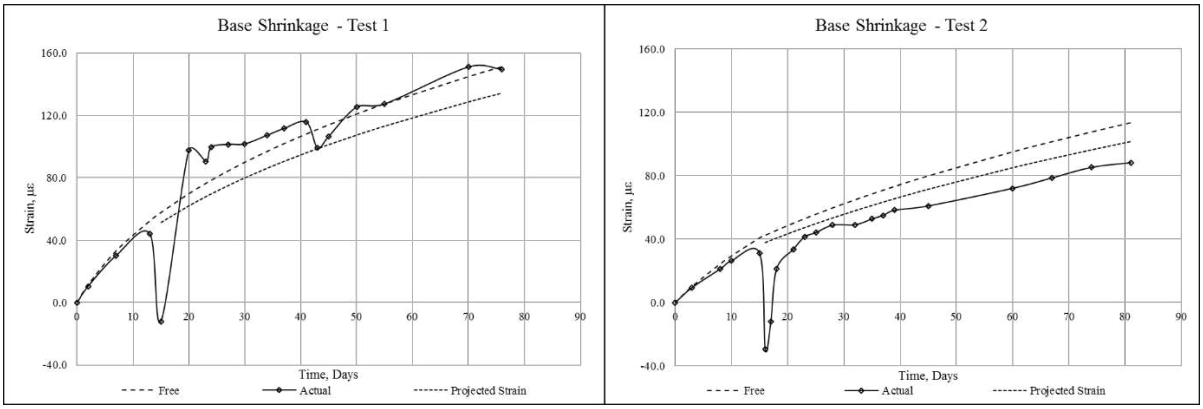

Figure 6. Influence of the wall on development of shrinkage in the base slab

3.4. Degree of Restraint

For the purpose of the restraint calculation, the wall was divided into middle (1600 mm) and edge regions (800 mm on either side). The degree of restraint is calculated by dividing the restrained strain by the unrestrained or free strain. The restraint at the edge and middle regions of the wall has been compared with that calculated for walls having the same aspect ratio using the ACI Committee 207 (12), BS EN 1992-3 (13) and from the work by Stoffers (5) and Schleeh (20) - Figure 7 shows the comparison of the stated restraint factors and the variation of restraint over the height of the wall. . From the tests it can be seen that the restraint is greater in the middle section of the wall and lower near the free ends of the wall. Also, due to the presence of the vertical steel reinforcement, the degree of restraint appears to be a lot greater at the joint between the two members. The experimentally obtained values of restraint vary considerably from the predicted values; for test 1 (no vertical steel) the degree of restraint is less, whilst in test 2 (vertical steel present) the restraint is greater. Figure 7 also suggests that the experimentally measured restraint decreases over the height of the wall, being maximum at the joint between the restrained and restraining members and minimum at the top of the wall. This decrease in restraint over the height of wall has also been mentioned by other researchers (3, 5, 7, 14, 15). Although Micallef (9) observed that the restraint is maximum at some point above the mid height of the wall and decreases towards the top and bottom of the wall. It can also be seen that the variation of restraint over the height of the wall is affected by the presence of vertical steel reinforcement. With time, the restraint over the height of wall decreases; in test 1, there was a significant loss of restraint over the height, whereas in test 2, the loss of restraint is comparatively lower. Previously (3, 7), it was believed that the loss of restraint over the height of a member is dependent on the height and aspect ratio of the members. However, these tests indicate that the amount of vertical steel reinforcement present in the wall also appears to contribute significantly to the degree of restraint at different points over the height and length of the wall. From Figure 7, it can also be seen that there is a change (reduction) in the gradient of the degree of restraint close to the top of the wall (middle section). It is thought that by preventing the base slab from curling, even though very little force was needed to do this, this may have induced a slight amount of tension near the top of the wall effectively reducing the restraint at this point.

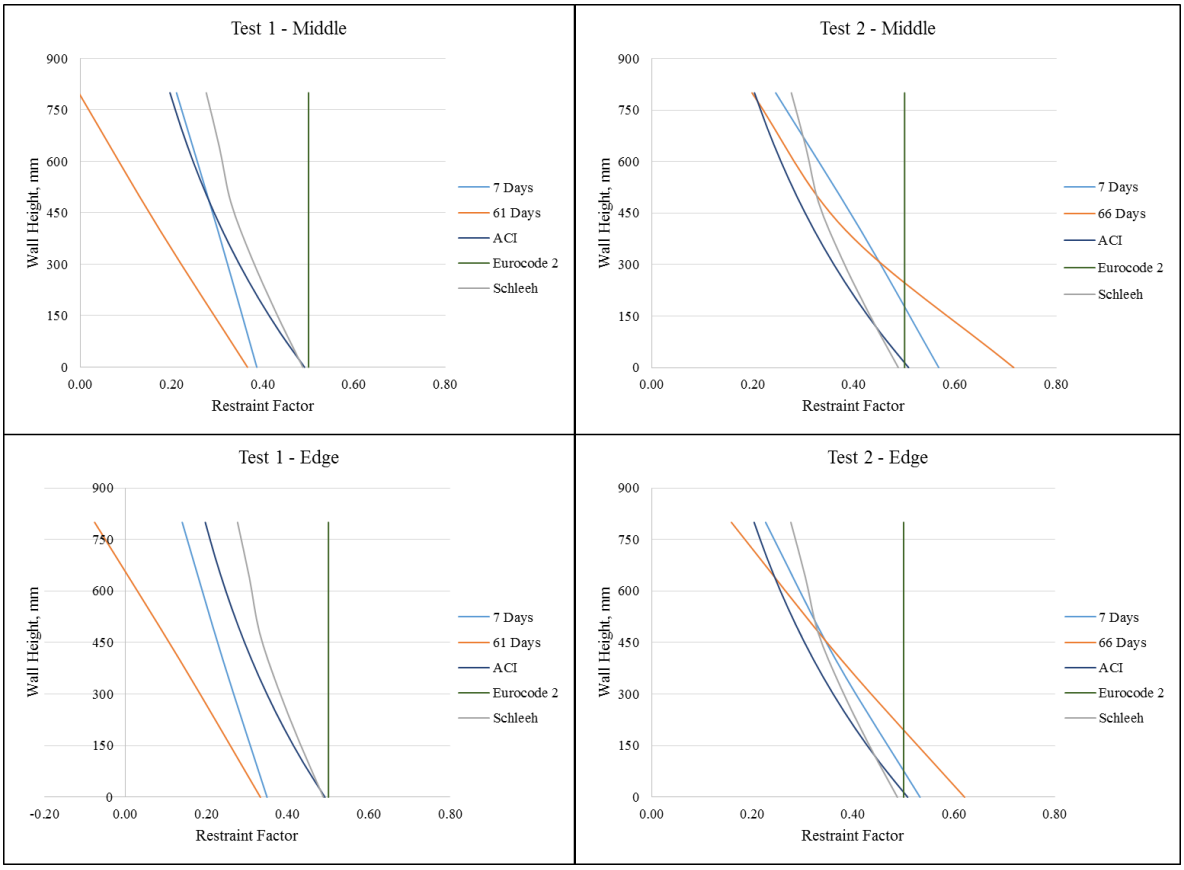

Figure 7. Variation of the degree of restraint along height; comparison of the experimentally obtained restraint factors with those estimated from the available guidance

Figure 8 illustrates the variation in the calculated degree of restraint at the joint with time. In test 1, the degree of restraint decreased with time; in test 2 it increased with time. Recently, experiments by Micallef (9) also revealed an increase in restraint with time; this they attributed to the loss of wall stiffness due to the occurrence of cracks. However, in the current study presented here, the degree of restraint increases with time in the presence of vertical steel dowels even when the wall did not exhibit any cracks. Also, even when cracks began to form after 51 days, there was no change to the gradient of increasing restraint with time (Figure 8). It is thought that the vertical reinforcement dowels provide an increased restraint to the ongoing shrinkage in both members and thus increase the value of the restraint factor. (The restrained strain in the base slab increases due to the steel bars and further augments the restrained strain present at the bottom of the wall.) In the absence of vertical reinforcement dowels (test 1), the time dependent shrinkage occurred without this restraint and the degree of restraint decreased with time. From these experimental results it can be seen that the degree of restraint decreased with time when $\rho_v = 0.07\%$ and increased when $\rho_v = 0.9\%$. This implies that within this range of vertical steel reinforcement, the degree of restraint may still decrease with time even if some

amount of vertical steel reinforcement is present. Further investigation is, therefore, required into the effect of vertical steel reinforcement ratio.

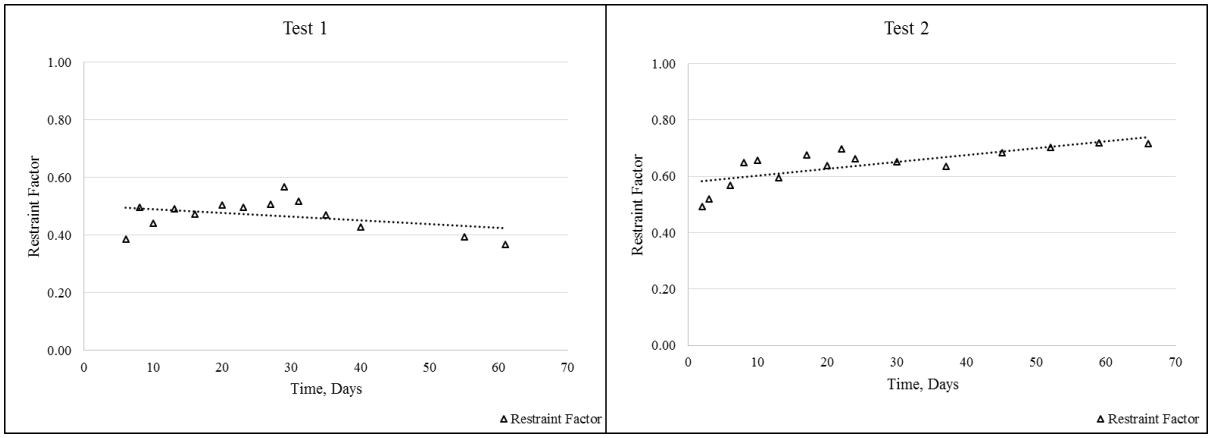

Figure 8. Experimentally obtained variation of the degree of restraint at the joint with time

3.5. Comparison of the Restrained Strain and Tensile Strain Capacity of Concrete

A comparison of the development of restrained strain and the tensile strain capacity (ε_{ctu}) of concrete with time is presented in Figure 9. The tensile strength and modulus of elasticity of the concrete were experimentally obtained at 28 days age and their development with time was estimated using the Eurocode expressions. From Figure 9, it can be seen that the tensile strain capacity of concrete, calculated by dividing the tensile strength by the modulus of elasticity, is exceeded during the first week after casting. However, in the experiments, no cracking was observed during this time; in fact, cracking occurred in test 2 only and in that too the first crack was witnessed during the 8th week after casting. Bamforth (3) in CIRIA 660 quoted the work by Tasdemir (24) and stated that the value of tensile strain capacity obtained from the ratio of tensile strength to the modulus of elasticity represents a lower bound value. The stresses caused in the concrete due to early age thermal and shrinkage effects represent a sustained loading and it was therefore suggested that the tensile capacity of concrete increases due to creep relaxation and a reduction in the failure stress due to the sustained loading. Figure 9 also compares the restrained strain with the tensile strain capacity calculated on the basis of the CIRIA 660 recommendations; interestingly, it was found that the restrained strain in the middle part of the wall exceeded the tensile strain capacity of the concrete 45 days after casting, which is almost similar to when the cracking in the wall was observed. Therefore, it is concluded that Eurocode 2 underestimates the development of the tensile strain capacity of the concrete and that the recommendations in CIRIA C660 for predicting the tensile strain capacity of the concrete are more reasonable. Although since the predicted crack was 6 days earlier than the crack observed

during the test, this suggests that the theory for tensile strain capacity, although appropriate, still needs some fine tuning.

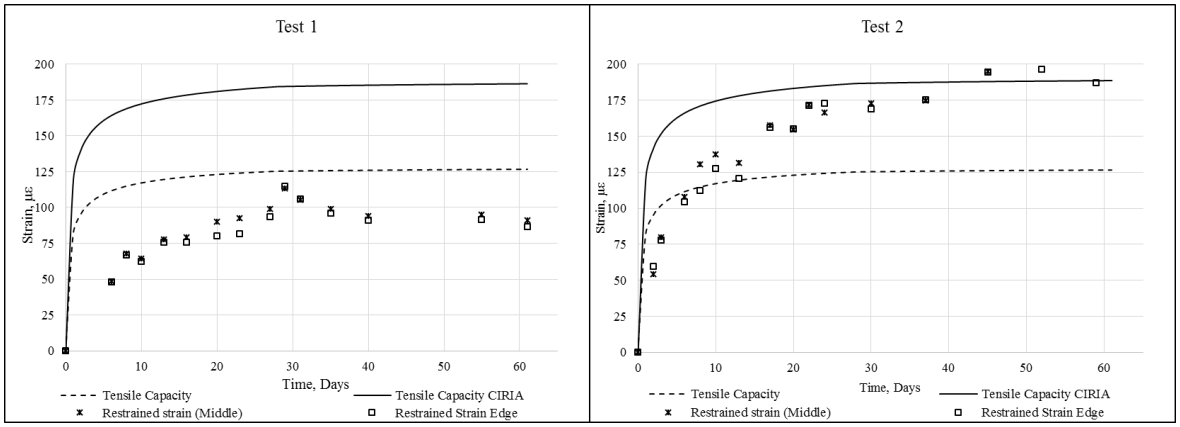

Figure 9. Comparison of the restrained strain and tensile strain capacity of concrete

3.6. Observed Cracking

At the start of this investigation, based on overall current theory, cracking due to the restraint of early age thermal and shrinkage imposed strains could be expected in the walls only a few days after casting. However, in the case of test 1, no cracking was observed during the entire duration of the test. In test 2, no cracks were observed during early ages, however, with time and an increase in the degree of restraint the first crack occurred 51 days after casting. The first crack formed on both faces of the walls at almost the same location along the length. The crack did not start at the joint, rather at 200 mm above the joint; it then propagated upwards and downwards over the wall height. Although it is generally perceived that cracking due to restrained volume changes is primarily caused by the restraint of early age thermal contraction, in this study it was apparent that the increase in restrained strain is continuous and drying shrinkage can also play an important role in the occurrence of cracks. After the appearance of the first crack, the wall was monitored for another four weeks during which time further cracks were formed. The four other small cracks appeared at different locations in the wall and are shown in Figure 10. These cracks were numbered, on both faces, according to the sequence in which they appeared. Like the first crack, cracks 2 and 4 also started a distance above the joint location and then propagated upwards and downwards. However, crack 3 and 5 on face 1 and crack 3 on face 2 initiated close to the joint and then propagated upwards. The fact that the cracks did not initiate at the joint can be attributed to the closing action of the base on the cracks as mentioned by Bamforth (3). The cracks observed in the walls did not propagate down to the joint between the wall and the restraining base and therefore the amount of load transferred to the base due to cracking could not be investigated. Crack widths (w_c) at different locations

along the crack were also measured using the portable microscope. Crack widths were seen to increase with time and the maximum crack width ($w_{c,max}$) was observed in crack 1; this was 0.3 mm on face 1, occurring 390 mm above the joint, and 0.24 mm on face 2, occurring at 375 mm above the joint. According to the findings of Kheder (7), Kheder, Al-Rawi (8) and Bamforth (3), the maximum crack width in an edge restrained wall occurs at a height of approximately 10% of the length of the wall which in this case is equal to 320 mm. The maximum crack width in the test occurred at a height between 11-12% of the wall length. This maximum value of crack width was reached in the second week after the initiation of the first crack and thereafter remained constant for the remaining duration of the monitoring period. Theoretically, the crack width was calculated using the theory given in BS EN 1992-1-1 (22). This gave the value of maximum crack width for the tested wall to be 0.13 mm, which is quite a lot less than the values obtained experimentally. It should also be noted that the degree of restraint at the point of initiation of the first crack was 0.55 and at the location of maximum crack width it was 0.39. However, the maximum value of the degree of restraint was 0.72 at the joint between the two members.

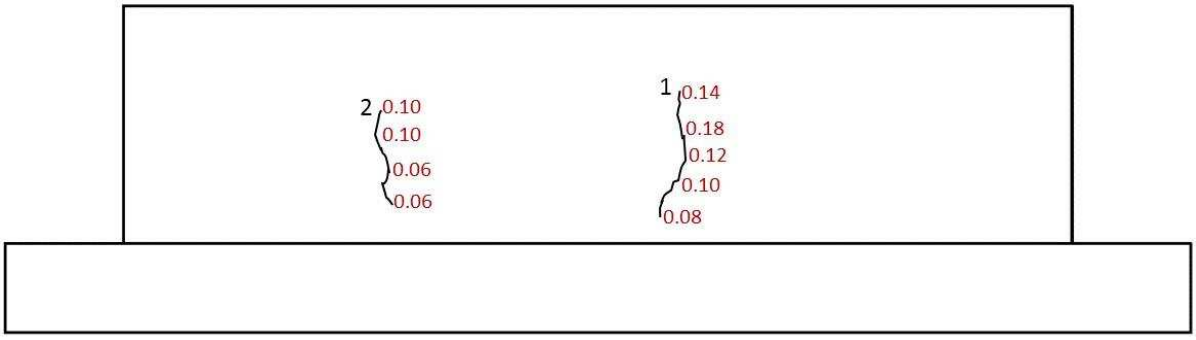

(a)

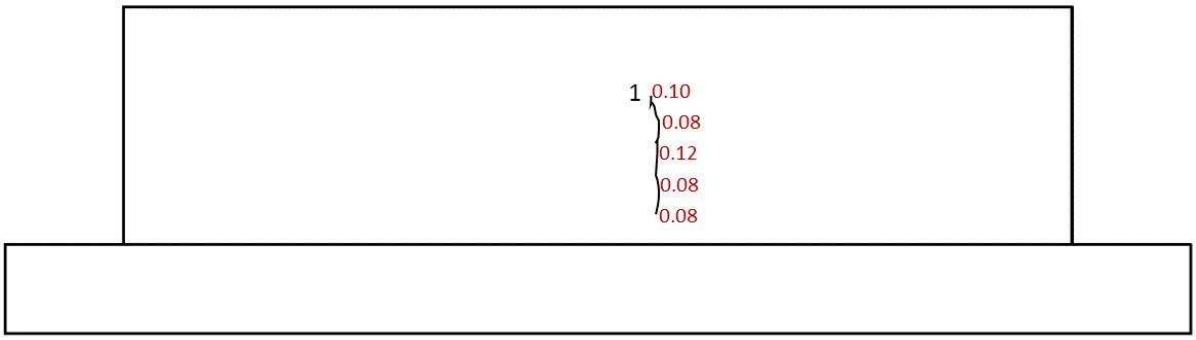

(b)

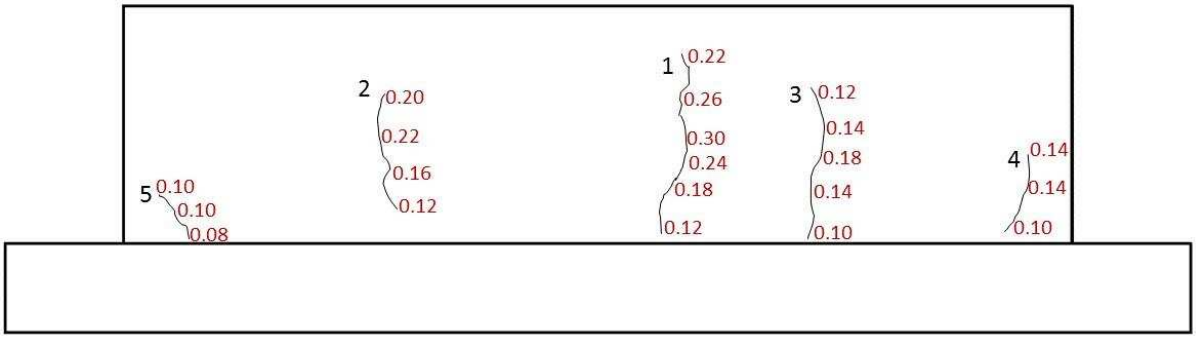

(c)

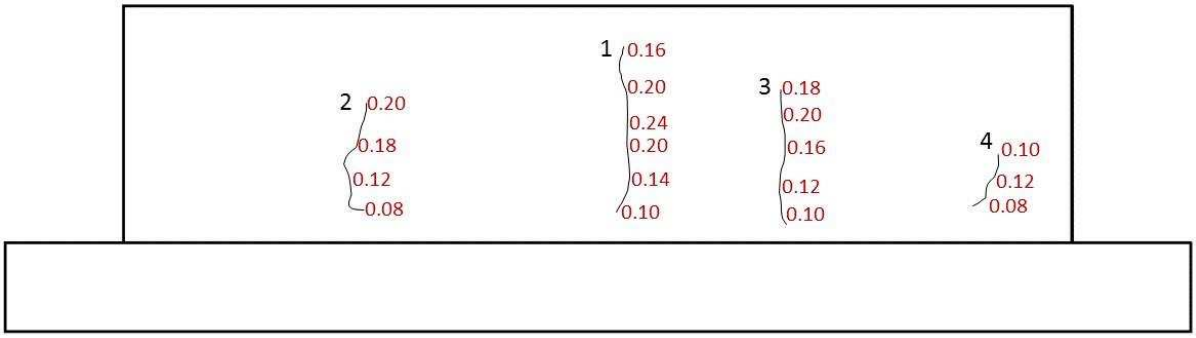

(d)

Figure 10. Observed cracking in the wall during test 2: (a) face 1 during 1st week; (b) face 2 during 1st week; (c) face 1 during 4th week; (d) face 2 during 4th week

4. Finite Element Analysis

4.1. Introduction

In light of the experimental results, finite element models were prepared and calibrated against the results obtained. The finite element analysis was performed using MIDAS FEA. Linear and Nonlinear static analysis were performed in MIDAS FEA for the above mentioned models.

4.2. Finite Element Modelling

In order to correctly simulate the experimentally obtained behaviour of the wall, and assess the effect of restraining any curling of the base, four different restraint conditions were modelled for both vertically reinforced and unreinforced walls and the results were compared to those obtained during the tests. Each wall was assigned a unique code for identification comprising a letter and a number; the letter U and R represent the walls ‘Unreinforced’ or ‘Reinforced’ with vertical steel reinforcement and the number indicates the support conditions as explained below:

a. Support condition 1. Wall was modelled with its bottom nodes fixed to represent total restraint.
b. Support condition 2. Wall and base slab were modelled and the bottom nodes of the base slab fixed to represent total restraint applied to the base slab.
c. Support condition 3. Wall, base slab and the floor were modelled such that the slab was connected to the floor using elastic links. This represented a partial restraint imposed on the base slab by the floor.
d. Support condition 4. Wall and floor were modelled such that the wall was connected to the floor using elastic links. The stiffness for the elastic link elements was determined from the experimentally observed behaviour of the base slab.

The wall, base slab and the floor were modelled using 20 noded three dimensional hexahedron solid elements (50mm). Figure 11 shows the finite element meshes used in the analysis for each type of support condition. In order to model the concrete, a total strain based cracking model involving a rotating crack model was used. The tensile behaviour of the concrete was modelled using the nonlinear function proposed by Hordijk (25), which provides a nonlinear softening curve for predicting the post cracking tensile behaviour of concrete assuming that the stress gradually reduces to zero at an ultimate strain, $\varepsilon_{ult} = 5.136\,(G_f^I/f_{ct}h_e)$, where G^I_f is the mode I fracture energy of concrete, h_e is the element size and f_{ct} is the concrete tensile strength. Fracture energy of the concrete was calculated according to the Model Code (23). The reinforcement was modelled using the embedded bar in solid elements, which assumes a perfect bond between steel and concrete and adds the stiffness of the reinforcement elements to the mother elements in the finite element formulation. Material properties were obtained from the experimental tests and used as input in the models. Time independent analysis were performed in which the materials properties were not varied with time. Taking advantage of the symmetry of dimensions, reinforcement, loads and boundary conditions, only a quarter of the wall was modelled in order to economize the computational effort. The thermal contraction and shrinkage observed in the walls during the experimental study were simulated using the thermal loads assigned as nodal temperatures to each element. The assigned temperatures were varied over the height and length of the wall as observed during the tests.

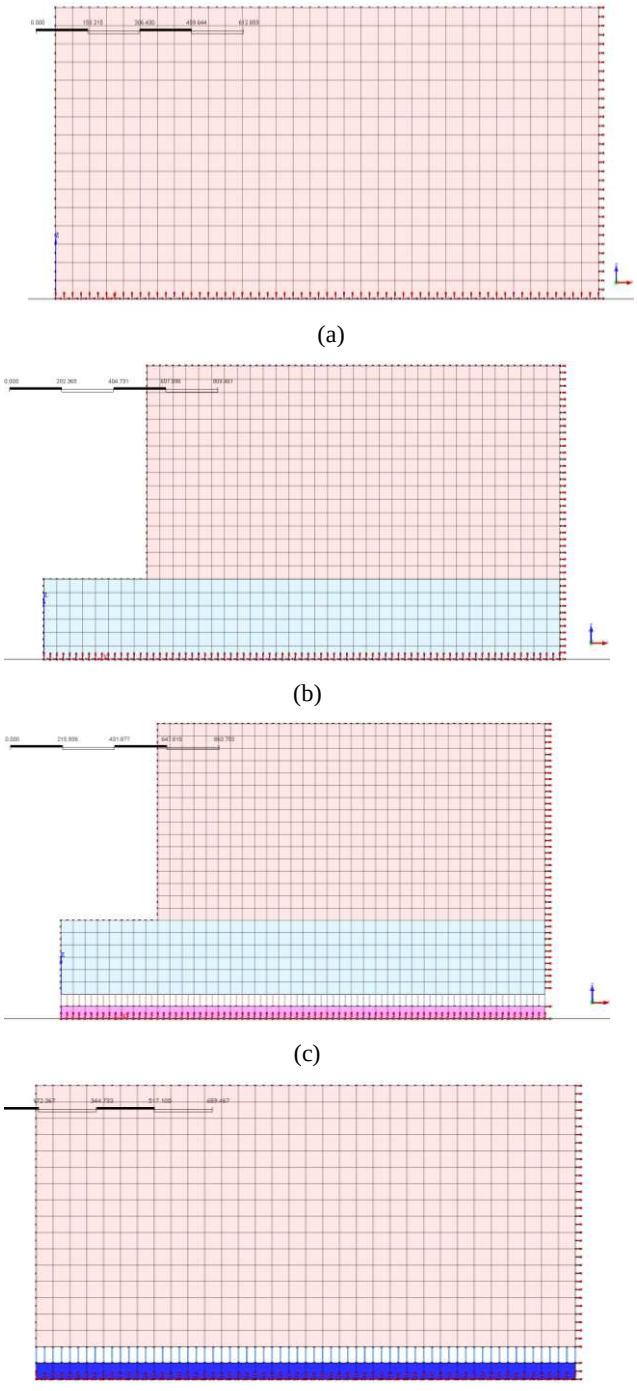

(a)

(b)

(c)

(d)

Figure 11. Finite element mesh used in the analysis: (a) support condition 1; (b) support condition 2; (c) support condition 3; (d) support condition 4

4.3. Finite Element Analysis and Results

The Newton Raphson iteration scheme was employed for obtaining the nonlinear solution in which the energy and displacement norms for a convergence tolerance of 0.001 were satisfied. Linear analysis was utilized for calculating the degree of restraint, whereas the cracking behaviour was observed from the nonlinear analysis. From the analysis results, it was

seen that with an increase in the thermal contraction, the stress increases in the wall; once the tensile stress exceeds the tensile cut off value, the crack appears. On the occurrence of a crack, the stress in the vicinity of the crack is seen to drop and with a further increase in contraction, the stress in the remaining parts of the member accumulates, resulting in another crack at a different location, which also relieves the stress locally. This is in line with the guidance provided by and Bamforth (3) with respect to the formation of cracks under edge restraint. The degree of restraint for each of the modelled cases was calculated using the obtained strain values. The degree of restraint over the height of wall obtained from the finite element analysis was compared with the values obtained experimentally (see Fig 12 (a) and (b) for test 1 and 2, respectively). The variation of the restraint with height was observed in all of the modelled scenarios. The degree of restraint obtained from the finite element analysis for case 1 and 2 exceeds the values obtained during the tests. The degree of restraint obtained for case 3 is important as it shows the effect of curling on the restraint profile. The profile of restraint matched the experimental values over the lower two thirds of the wall, however, near the top the software predicted less restraint as a small amount of compression will be induced at this point from the curling (compare this with the experimental values where the restraint measured tended to increase near the top due to the induced tension from not permitting curling to occur). Case 4 predicts the variation of restraint over the height reasonably well for both tests. The finite element study presented in this section also, therefore, highlights the importance of correctly simulating the actual support conditions -it is not appropriate to consider the wall or the base slab edge totally restrained from movement and the mechanism supporting the base slab needs to be incorporated in the finite element analysis. In practice, when the base slab is cast on soil, soil structure interaction may be modelled using the springs incorporating the modulus of subgrade reaction of the soil. However, since the tests in the present study were conducted in the laboratory and the slab was cast on the laboratory strong floor, and a special clamping mechanism was used to prevent the development of curvature in the slab, the use of elastic links for simulating the behaviour of the base slab appeared to be an appropriate option.

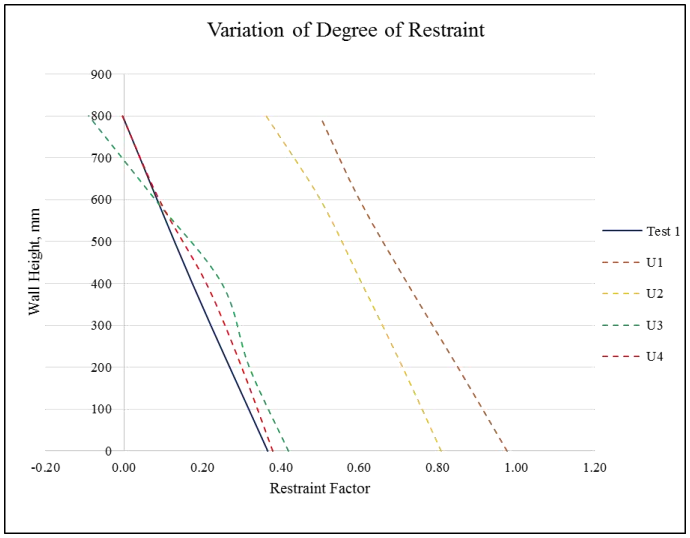

(a)

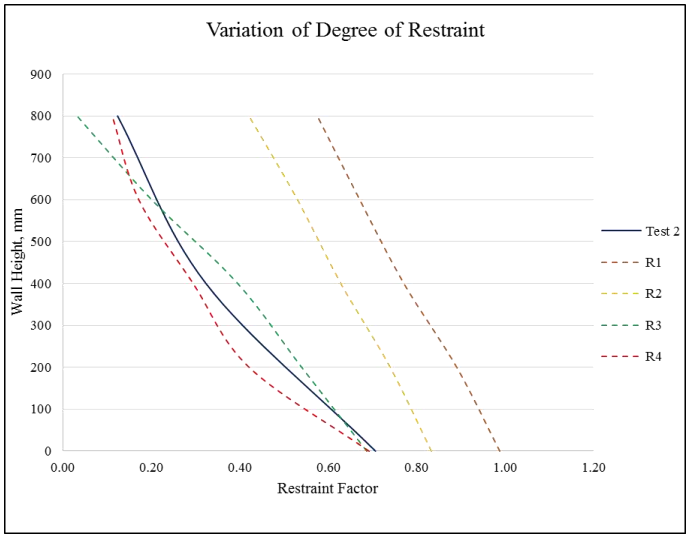

(b)

Figure 12. Comparison of experimentally obtained restraint factors with those obtained using the finite element analysis: (a) comparison with test 1; (b) comparison with test 2

Owing to the different support conditions, the strain profile / cracking behaviour of each modelled wall was also different, despite having similar loading and material properties. Finite element models U3 and U4 did not develop any cracks, however, in the case of walls U1 and U2, cracks were formed as indicated in the strain profiles for each of the U-series walls in Figure 13. Formation of these cracks is obviously contrary to the experimental findings and is attributed to the applied boundary conditions simulating a total restraint. In the case of the R-series walls, each of the modelled walls developed cracks, as shown by the strain profiles in Figure 14. An unrealistic depiction of total restraint in walls R1 and R2 induced full height cracks whereas, in the case of walls R3 and R4, in which the elastic links were used, the developed cracks did not propagate over the full height of the wall. The cracks that developed in wall R4 can be related to those obtained in test 2 in which the first crack appeared close to

the centre of the wall and, with an increase in the thermal contraction, the second crack appeared in between the free end and the first crack. Wall R4 predictions bear close resemblance to the cracks obtained in test 2 except that no crack can be seen close to the free end of the modelled wall. It is anticipated that the adopted experimental methodology of clamping the base slab to the floor induces tensile stresses near the free ends of the wall which led to the crack forming close to the ends. From the cracking patterns and the restraint variations obtained using the finite element models, it can be inferred that modelling of the real time support conditions has a significant importance.

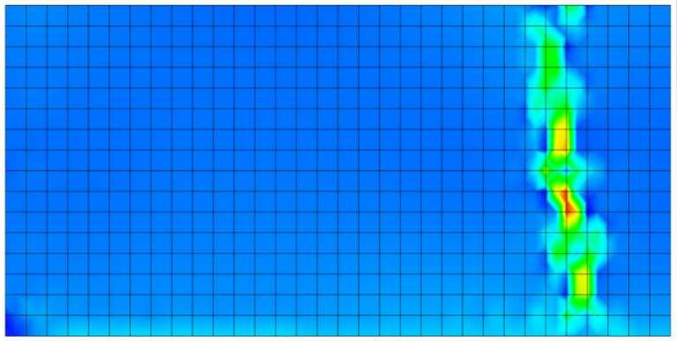

(a)

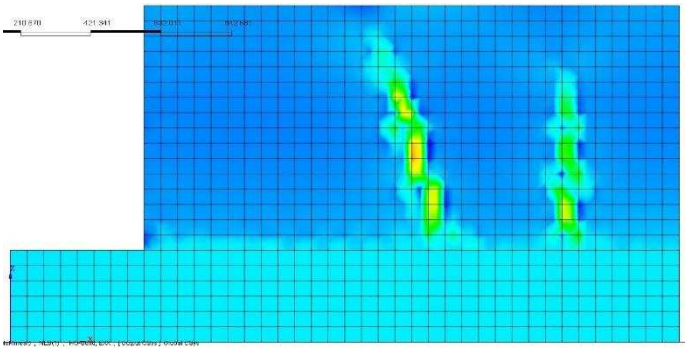

(b)

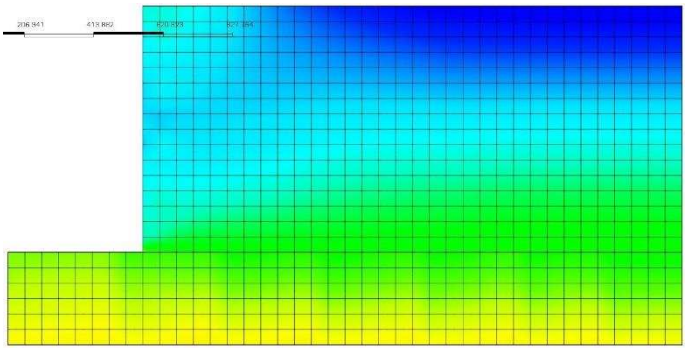

(c)

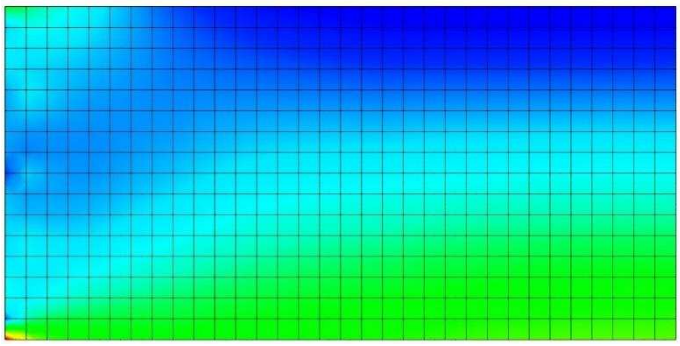

(d)

Figure 13. Strain profile of U-series wall obtained using the finite element analysis: (a) wall U1; (b) wall U2; (c) wall U3; (d) wall U4

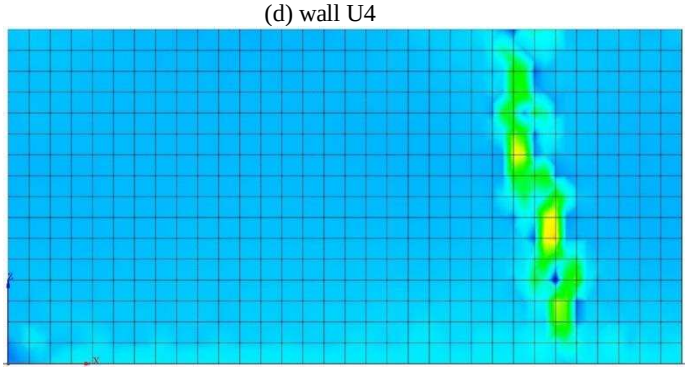

(a)

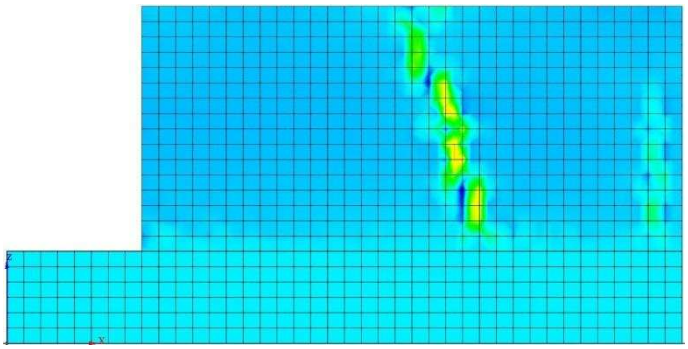

(b)

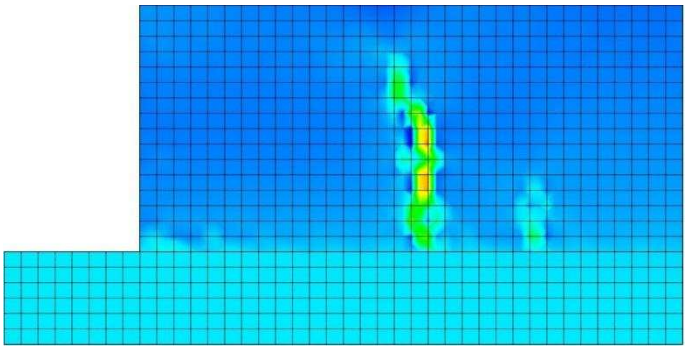

(c)

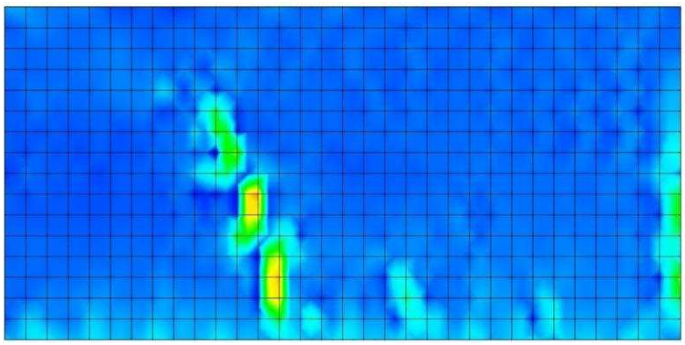

(d)

Figure 14. Strain profile of R-series wall obtained using the finite element analysis: (a) wall R1; (b) wall R2; (c) wall R3; (d) wall R4

5. Conclusions

This investigation provides sufficient evidence to suggest that:

a. The vertical steel reinforcement present at the joint between the restraining base and the edge restrained wall has a significant impact on the degree of restraint to imposed strains. This increase in restraint, also with time, suggests that the current guidance is flawed.
b. To fully understand the mechanism of edge restraint it is necessary to quantify the thermal exchanges between the wall and the base - this can only be done when using a concrete base; experimental investigations using steel bases are misleading and inappropriate.
c. As recommended by Bamforth (3), the stresses induced due to early age thermal and shrinkage effects represent sustained loads and under these loads the tensile strain capacity of the concrete increases.
d. Drying shrinkage can play a significant role in the development of cracks.
e. Maximum crack width does not occur at the location of maximum restraint; this occurs at some height above the joint location with cracks propagating both upwards and downwards.
f. When estimating the degree of restraint imposed on the wall, it is important to take into account the real base support conditions.
g. The current guidance still potentially underestimates the T_1 values – CIRIA C660 predicts 30 ºC; the measured value was 33 ºC. However, it could be viewed that the CIRIA value is still conservative as if the temperature heating and cooling profile is compared directly with the time-dependent change of compression to tension in the section, the stage that the section theoretically goes into tension is at a temperature

below peak temperature, so it is logical not to measure temperature drop from peak temperature.

References

1. Forth JP, A.J. Martin. Design of Liquid Retaining Concrete Structures. Third ed. UK: Whittles Publishing; 2014. 175 p.

2. Emborg M, Bernander S. Assessment of risk of thermal cracking in hardening concrete. Journal of Structural Engineering. 1994;120(10):2893-912.

3. Bamforth P. Early-age thermal crack control in concrete: CIRIA; 2007.

4. Evans E, Hughes B, editors. SHRINKAGE AND THERMAL CRACKING IN A REINFORCED CONCRETE RETAINING WALL. ICE Proceedings; 1968: Thomas Telford.

5. Stoffers H. Cracking due to shrinkage and temperature variation in walls: Stevin Laboratory, Department of Civil Engineering, Delft University of Technology and IBBC Institute TNO for Building Materials and Building Structures; 1978.

6. Kheder G, Al Rawi R. Control of cracking due to volume change in base-restrained concrete members. ACI Structural Journal. 1990;87(4).

7. Kheder G. A new look at the control of volume change cracking of base restrained concrete walls. ACI structural journal. 1997;94(3):262-71.

8. Kheder G, Al-Rawi R, Al-Dhahi J. A study of the behaviour of volume change cracking in base restrained concrete walls. Materials and Structures. 1994;27(7):383-92.

9. Micallef M, Vollum, RL, Izzuddin, BA. Crack development in transverse loaded base-restrained reinforced concrete walls. Engineering Structures. 2017;143:522-39.

10. Beeby and Forth. Control of cracking in walls restrained along their base against early thermal movements. Concrete for Transportation Infrastructure. 2005.

11. Bamforth P, Denton, S, Shave, J. The development of a revised unified approach for the design of reinforcement to control cracking in concrete resulting from restrained contraction. ICE Research project. 2010;706.

12. ACI Committee 207. Effect of restraint, volume change, and reinforcement on cracking of mass concrete. ACI Materials Journal. 2007;87(3).

13. BS EN 1992-3. Eurocode 2: Design of Concrete Structures: Part 3: Liquid retaining and containment structures: British Standards Institution; 2006.

14. Nilsson M. Restraint factors and partial coefficients for crack risk analyses of early age concrete structures: Luleå University of Technology; 2003.

15. Carlson RW, Reading TJ. Model Study of Shrinkage Cracking in Concrete Building Walls. Structural Journal. 1988;85(4).

16. Emborg M. Thermal stresses in concrete structures at early ages: Luleå tekniska universitet; 1989.

17. BS 8007. Code of practice for Design of concrete structures for retaining aqueous liquids. BS 8007. British Standards Institute, London. 1987.

18. BS 8110-2. Structural use of Concrete–Part 2: Code of practice for special circumstances. Reprinted incorporating amendments Nos 1 and. 1985;2:8110-2.

19. Klemczak B, Knoppik-Wróbel A. Comparison of analytical methods for estimation of early-age thermal-shrinkage stresses in RC walls. Archives of Civil Engineering. 2013;59(1):97--117.

20. Schleeh W. Die Zwangspannungen in einseitig festgehaltenen Wandscheiben. Beton- und Stahlbetonbau. 1962;57(3):64-72.

21. Concrete Society Technical Report. Concrete Society Technical Report. 2008 Contract No.: 67.

22. BS EN 1992-1-1. Eurocode 2: Design of Concrete Structures: Part 1-1: General Rules and Rules for Buildings: British Standards Institution; 2004.

23. Model Code CF. Fib model code for concrete structures 2010. Document Competence Center Siegmar Kästl eK, Germany2010.

24. Tasdemir M. The tensile strain capacity of concrete. Magazine of Concrete Research. 1996;48(176):211-8.

25. Hordijk DA. Local approach to fatigue of concrete: TU Delft, Delft University of Technology; 1991.